LARGE AREA SEA MAPPING WITH GROUND-IONOSPHERE-OCEAN-SPACE (GIOS)

Paul A. Bernhardt, Stanley J. Briczinski, Carl L. Siefring

Plasma Physics Division, Naval Research Laboratory, Washington DC, 20375, USA.

Donald E, Barrick, Calvin Teague

CODAR Ocean Systems, 1914 Plymouth Street, Mountain View, California 94043 USA

Jehu Bryant, Raytheon IIS, Chesapeake, VA

Andrew Howarth, Gordon James, Greg Enno, Andrew Yau

University of Calgary, Institute for Space Research Calgary, AB, T2N 1N4, CANADA

Large Area Ocean Measurements

- HF Ocean Scatter to Satellite
- Factors in Ground/Ionosphere/Ocean/Satellite (GIOS) Model
- Ocean Scatter Components
  - Wave Height Spectrum and Shoaling
  - Fresnel Area Contributions Inside Pulse Illumination Area
  - Skip Distance Caustic
  - Incident and Scattered Polarizations
- Observation Satellites (ePOP)
  - ROTHR Virginia Data with ePOP
  - Features in RTI Spectrum
- Future Measurements - CARINA
- Conclusions

Comparison of Ocean Measurement Techniques

- Passive Microwave Imagery
  - Ocean Microwave Emissivity
  - Surface Waves and Foam
  - Temperature and Salinity
  - Wind Speed and Direction
- Ocean Radars
  - Ground Surface Wave HF Radars – CODAR and WERA
    - Backscatter
    - Wind Speed and Currents
  - Microwave Scatterometers
  - Altimeters for Topography
  - GPS/GNSS Satellite Receivers for Reflectometry
  - Imaging Radars (SAR)
- Advantages of HF GIOS System
  - Large Area Coverage
  - HF Penetration of Dense Rain in Hurricanes
  - Measurement Resolution Matches Computer Models

Cyclone Global Navigation Satellite System (CYGNSS) Wind Speed Retrieval (Adapted from *Cinzia Zuffada, et al., JPL)*

- 8 Low Earth Orbit Satellites with GPS L-Band Receivers
- Wind Speed from Delay Doppler Mapping (DDM) and Geophysical Model Function (GMF)
- Wind Speed Uncertainty 2 m/s from UK-DMC data (*Gleason, 2013, Clarizia et al., 2014*) and TechDemoSat-1 data (*Foti et al., 2015*);
- Predicted Wind Speed Uncertainty for CYGNSS is 2 m/s or 10% of Measured Wind (*Clarizia and Ruf, 2015*);

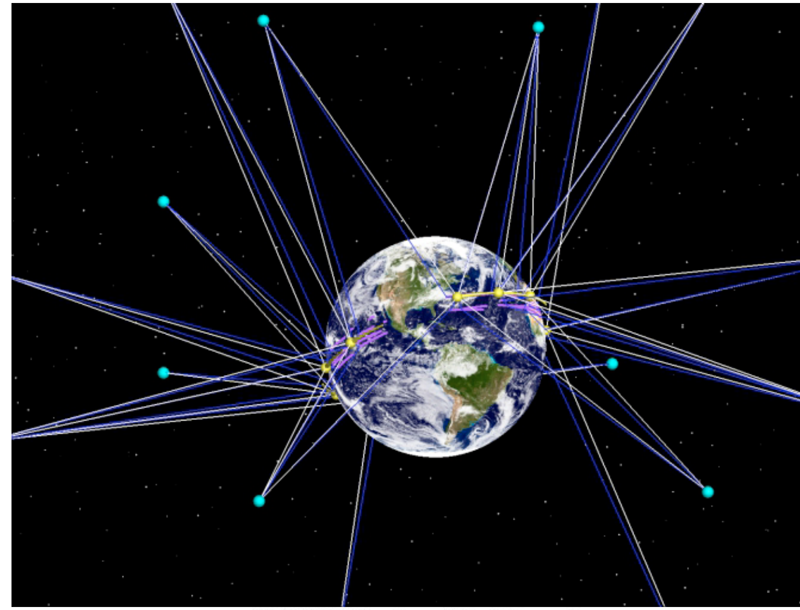

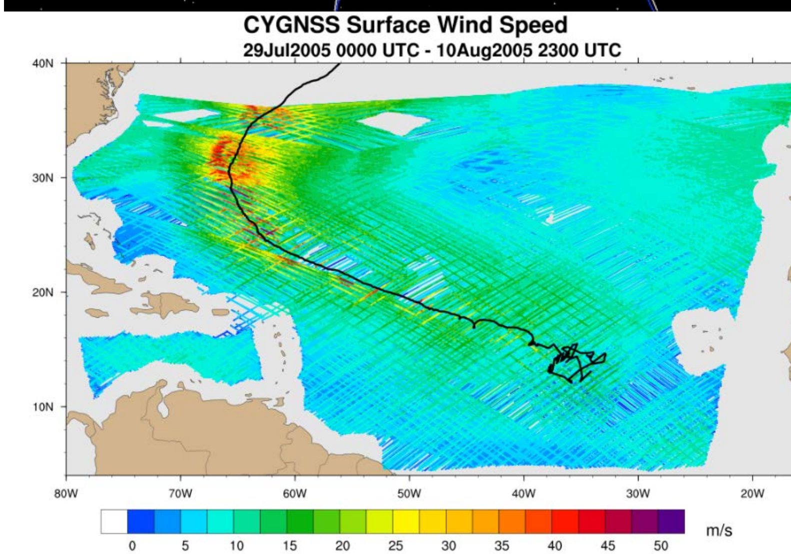

Example of true vs retrieved wind speed for CyGNSS Transect crossing the hurricane eye

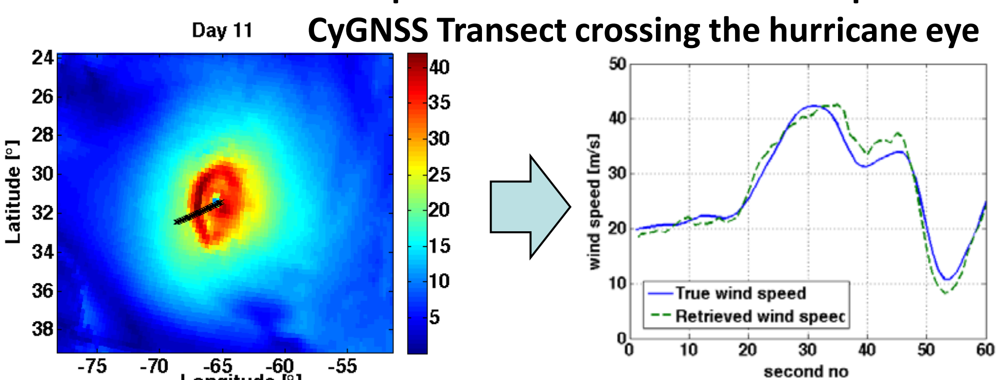

Ground-Ionosphere-Ocean-Space (GOIS) HF Transmitter *Sky-Wave* Scatter to Low Earth Orbit Satellites

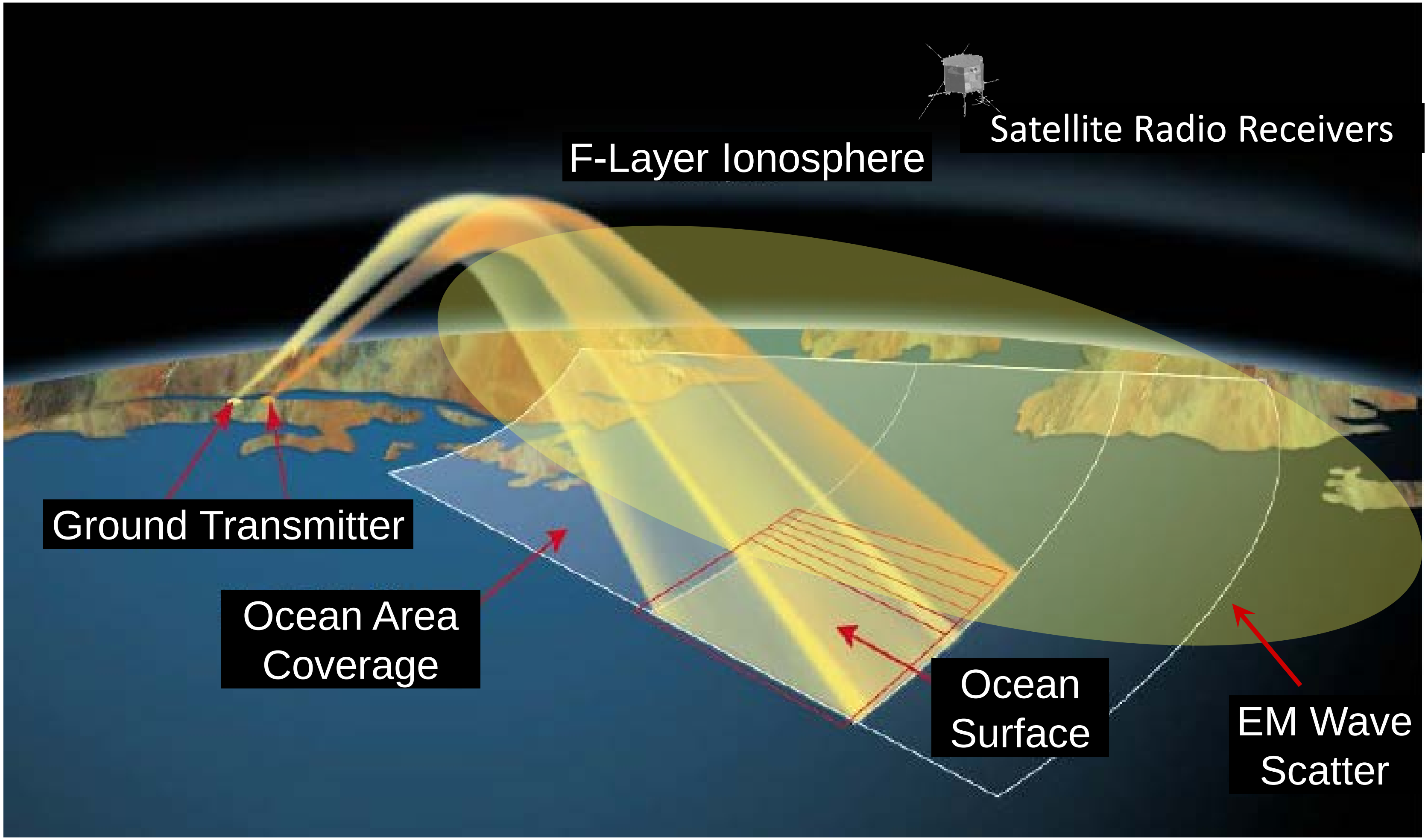

Great Improvement: HF Scatter to Satellite-Receiver Provides Large Area Coverage

HF Propagation Paths in Highly Structured Ionosphere

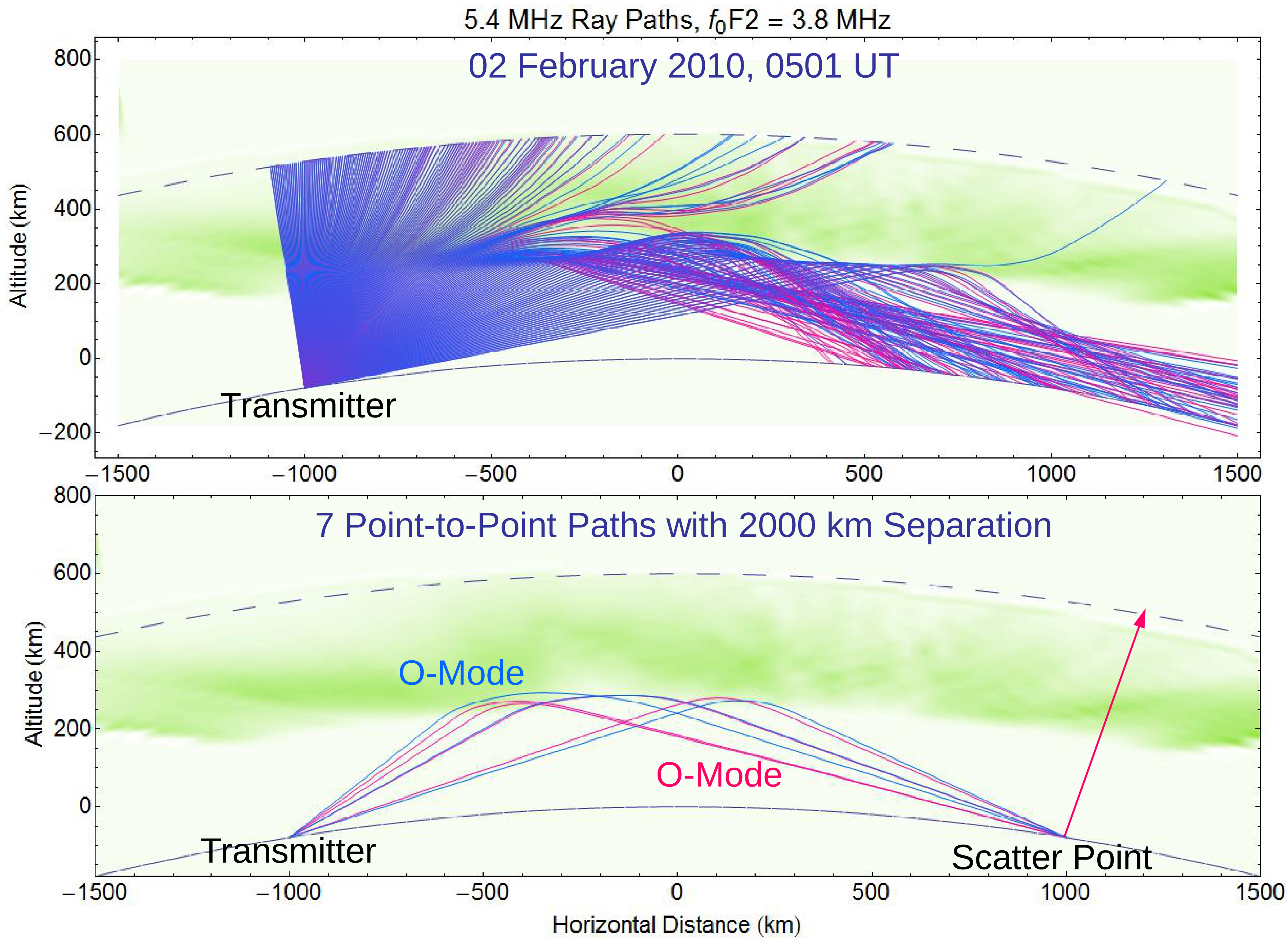

Ray Propagation Modes to Satellite with Single F-Layer

- O-Mode (LHCP Polarization) and X-Mode (RHCP Polarization) Propagation
- O ↔ X Mode Change for Specular Scatter while Bragg Scatter Retains Polarization
- Ocean Illumination Region, Incidence and Scatter Angles Shift with Satellite Position

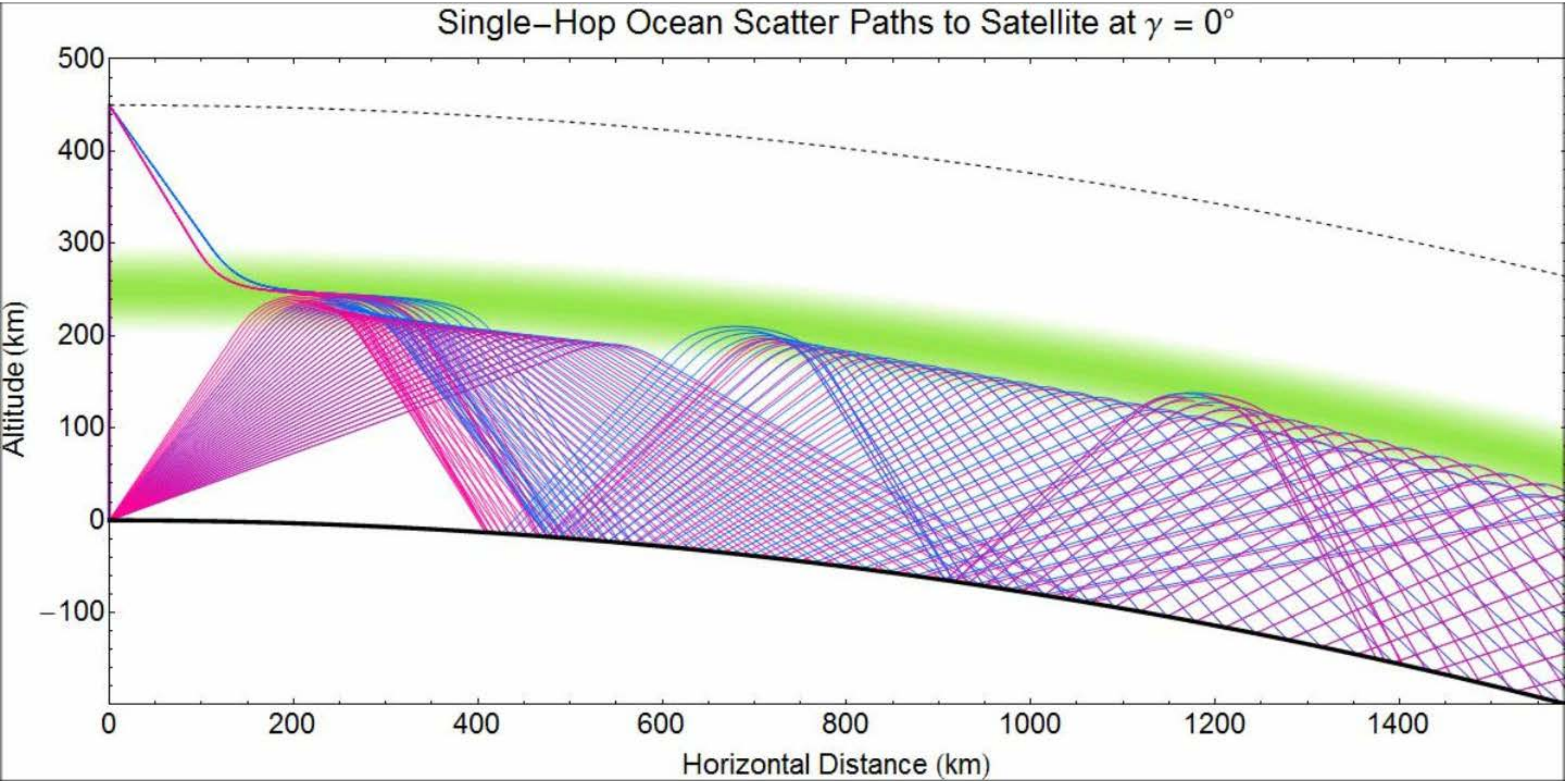

Ocean Surface Scatter Modes IV

- Total Scatter Component from Slightly Rough Surface
  - Sum of Coherent and Incoherent Scatter by Peake and Barrick [1967]
  - Fresnel Zone Scatter Area [Beckmann and Spizzichino, 1963]

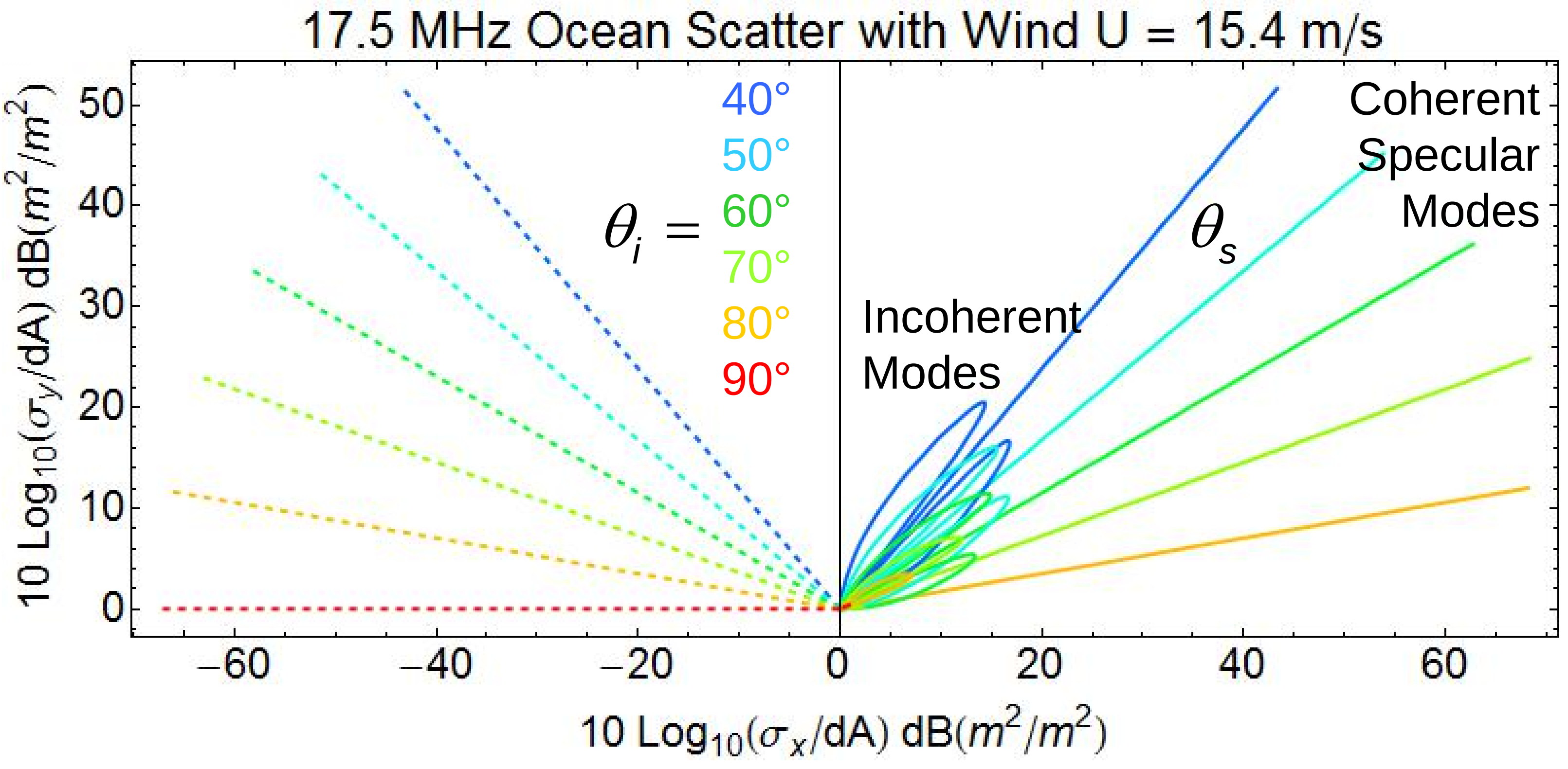

Specular Reflections from Land and Sea

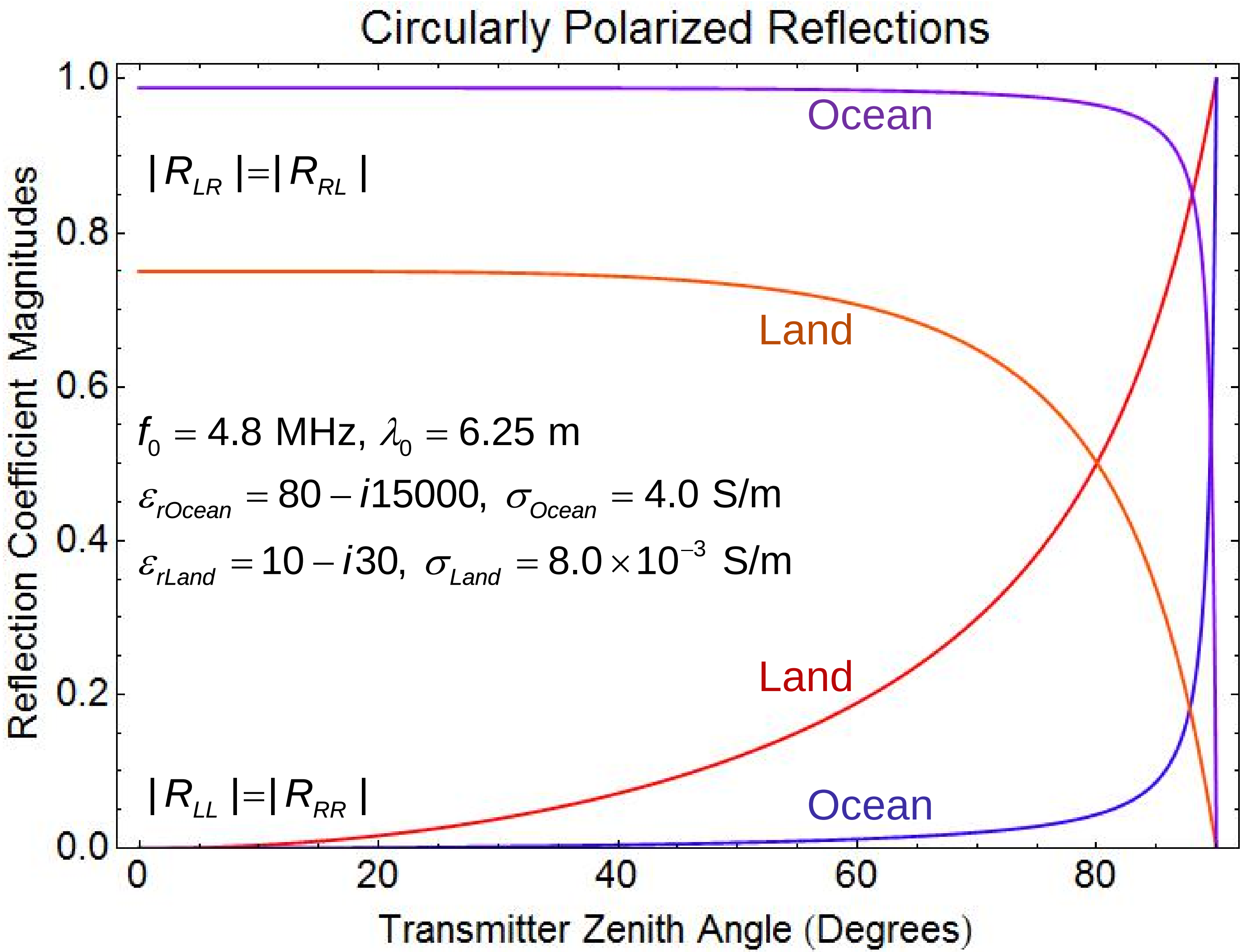

1^{st} Order Bistatic Ocean Scatter Theory (Barrick 1972)

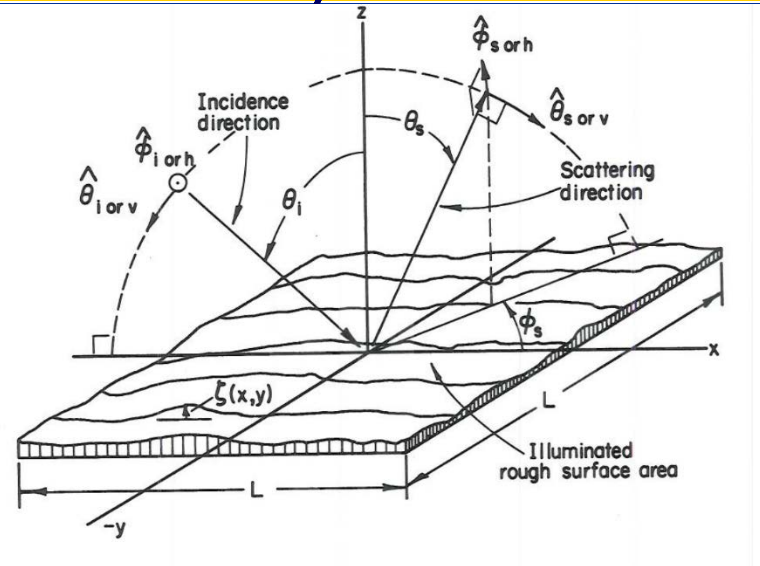

- Transmitted Wave
  - Wave Number $k_0 = 2\pi / \lambda$
  - Power P_T
  - Antenna Gains G_T, G_R
- Polarized Radar Cross-Section

$$\sigma_{ab}(\omega) = 4\pi k_0^4 P_{ab} 2^3 S[k_0(\sin\theta_s \cos\varphi_s - \sin\theta_i), k_0 \sin\theta_s \sin\varphi_s, \omega - \omega_0]$$

$$P_{vv} = (\sin\theta_i \sin\theta_s - \cos\varphi_s)^2, P_{vh} = \cos^2\theta_i \sin^2\varphi_s, P_{hv} = \cos^2\theta_s \sin^2\varphi_s, P_{hh} = (\cos\theta_i \cos\theta_s \sin\varphi_s)^2$$

- Wave Height Spectrum $S(\kappa_x, \kappa_y, \omega)$
  - Gravity Wave Dispersion $(\omega^+)^2 = g\sqrt{\kappa_x^2 + \kappa_y^2}$
  - First Order Spectrum $S(\kappa_x, \kappa_y, \omega) = S(\kappa_x, \kappa_y)\delta(\omega - \omega^+)$
  - Mean Square Wave Height $h^2 = \int_{-\infty}^{\infty}\int_{-\infty}^{\infty} S(\kappa_x, \kappa_y) d\kappa_x d\kappa_y$
  - One Dimensional Temporal Spectrum $S(\omega) = \int_{-\infty}^{\infty}\int_{-\infty}^{\infty} S(\kappa_x, \kappa_y)\delta(\omega - \omega^+) d\kappa_x d\kappa_y$
- Radar Equation $dP_R(\omega) = \dfrac{P_T G_T G_R \lambda^2}{(4\pi)^3 R_R^2 R_T^2} dS\sigma(\omega)$ $\quad \dfrac{W}{rad / s}$

Wave Height Wave Number Spectrum
Derived from Puerto Rico Wave Buoy Data

Source: http://www.ndbc.noaa.gov/station_page.php?station=XXXXX

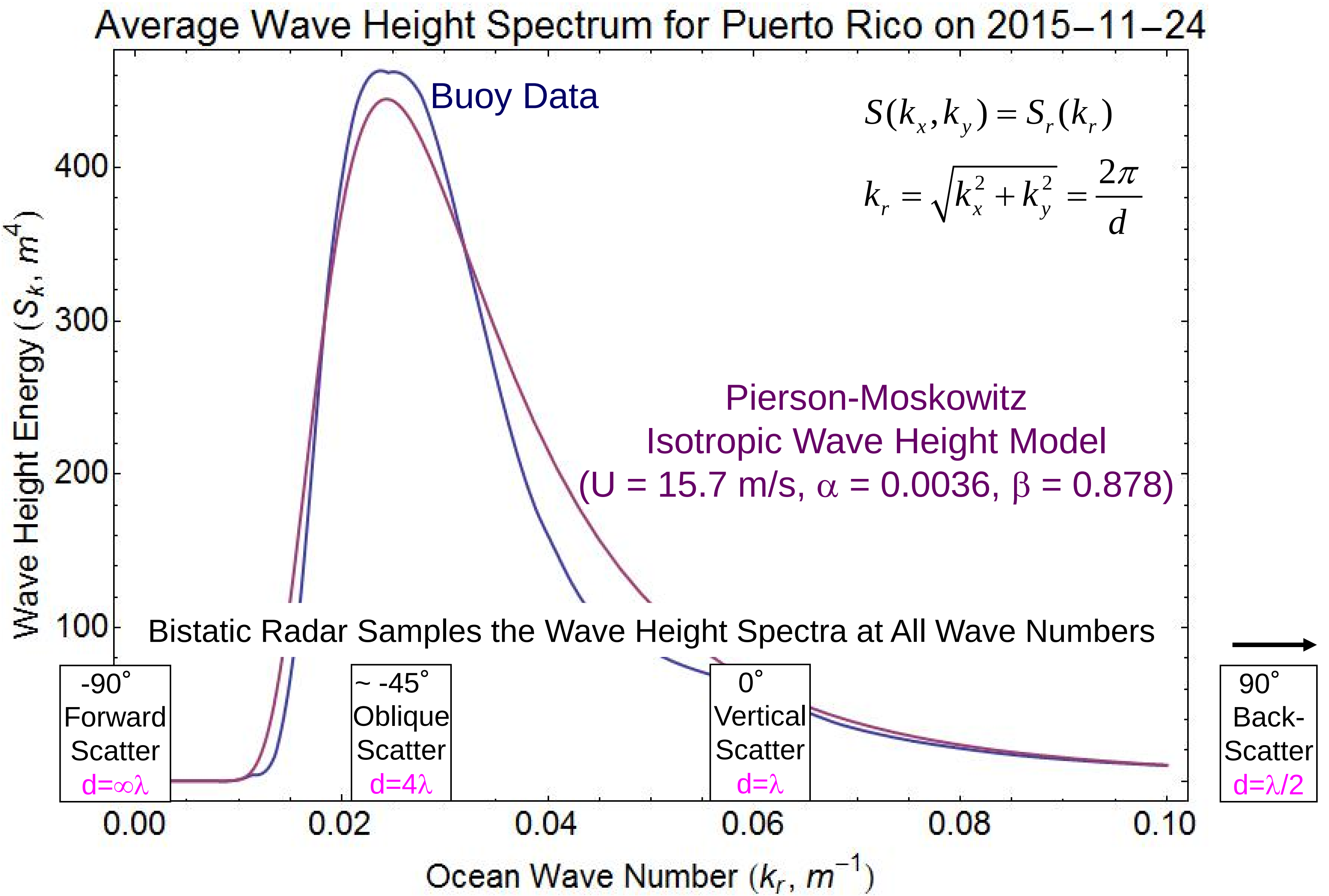

Shoaling Influence on Wave Frequency Shifts and Amplitude Increases for Wave Number Spectra

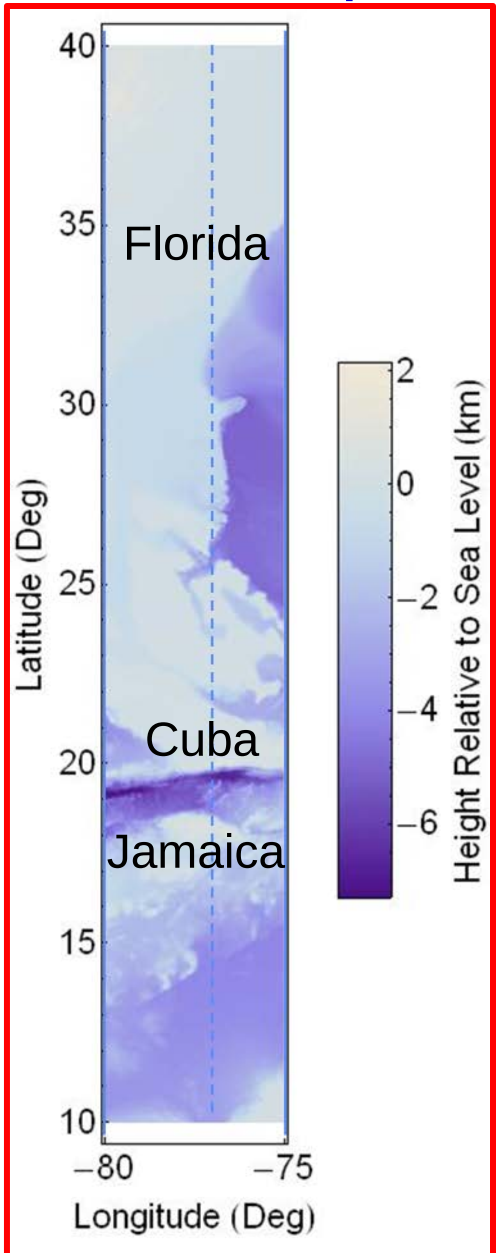

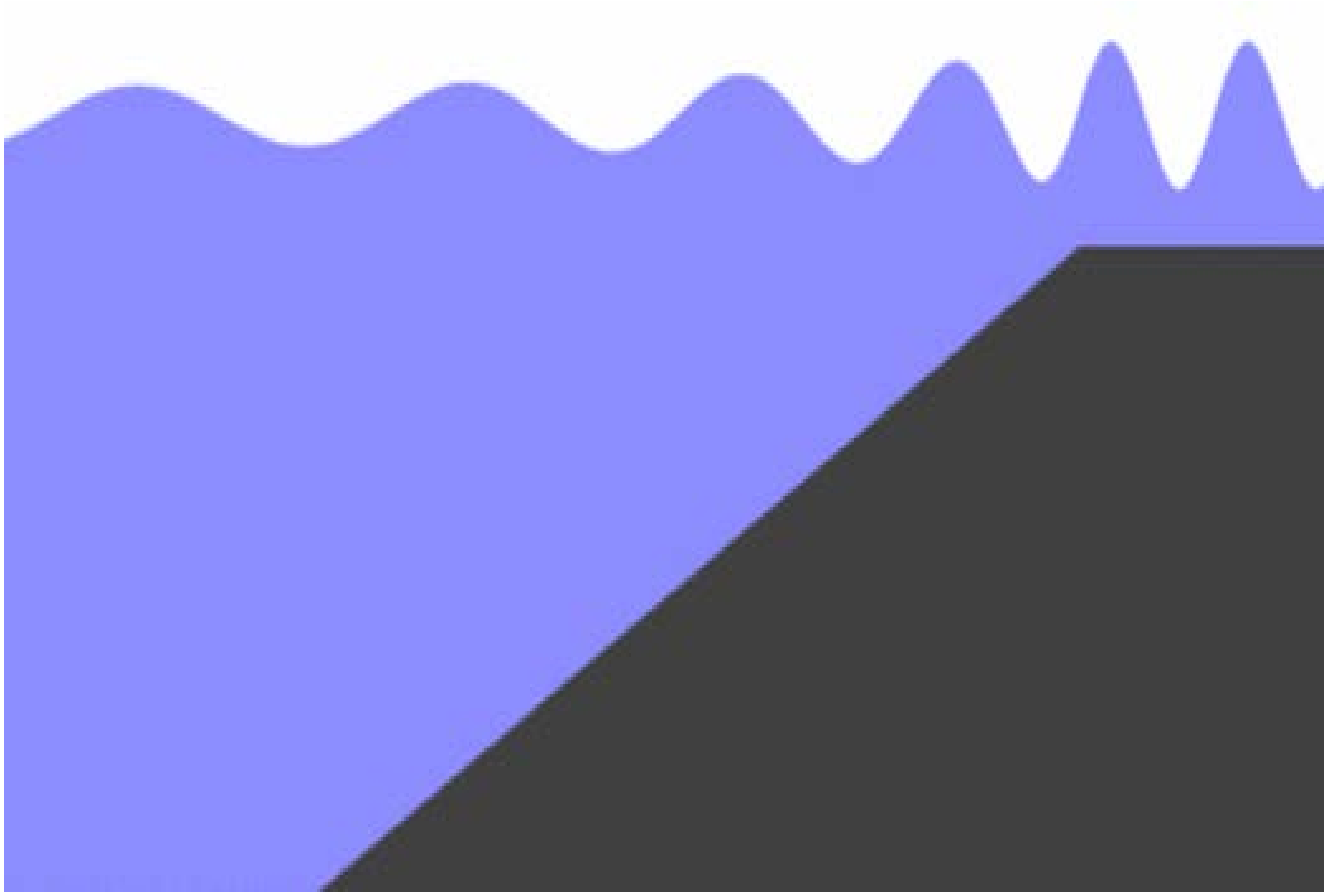

GOIS Mapping of Arctic Sea-Ice Transitions

Photo from R/V Lance before wave event, 2010 May 2, 15:48 UTC

Collins, C.O., W. E. Rogers, A. Marchenko, and A. V. Babanin (2015), In situ measurements of an energetic wave event in the Arctic marginal ice zone, *Geophys. Res. Lett*., **42**.

Broken ice: negligible damping of dominant waves

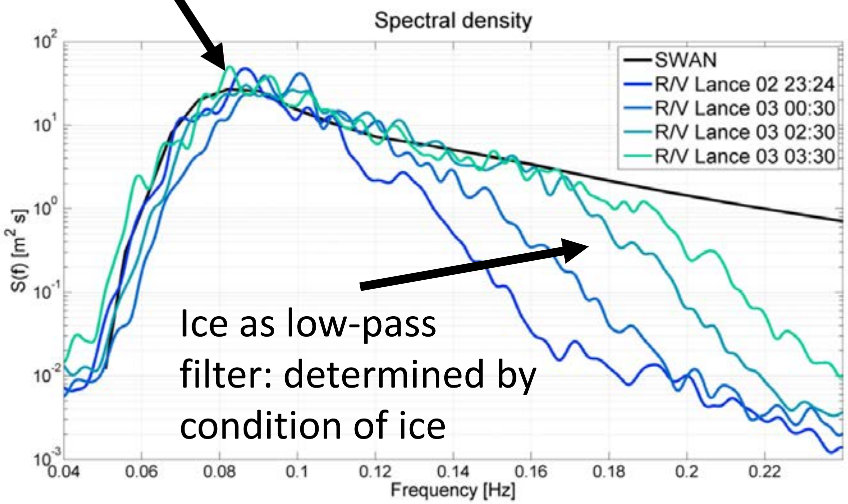

[Fig. 4] The evolution of *S(f)* over the course of 5 hours as the ship encountered smaller ice floes. The first spectra is shown in dark blue and later spectra transitioning to aqua. SWAN spectra at this time, with no ice representation, is shown in black for reference.

Factors Affecting Scattered HF Power to Satellite

- Transmitter Power and Antenna Gain
- Ray Path Spreading
  - Transmitter to Ionosphere
  - Ionosphere to Ocean
- Scattering from Ocean
  - Wave Number Spectrum of Ocean Wave Height
    - Wind Velocity
    - Ocean Depth and Shoaling (Wave Growth in Shallow Water)
    - Ocean Current
  - Polarization of Incident and Reflected HF Wave
  - Scatter Coefficient, σ_0
    - Specular/Coherent Scatter
    - Incoherent/Bragg Scatter
  - Fresnel Zone Area ($\Delta_{Phase} < \lambda/2$) < Illuminated Area $T_P\ C\ \Delta\phi\ R$
- Ray Path Spreading and Refraction to Satellite

Fresnel Zone Size and Illumination

Ellipse in Reflecting Plane < λ/2 HF Phase Change

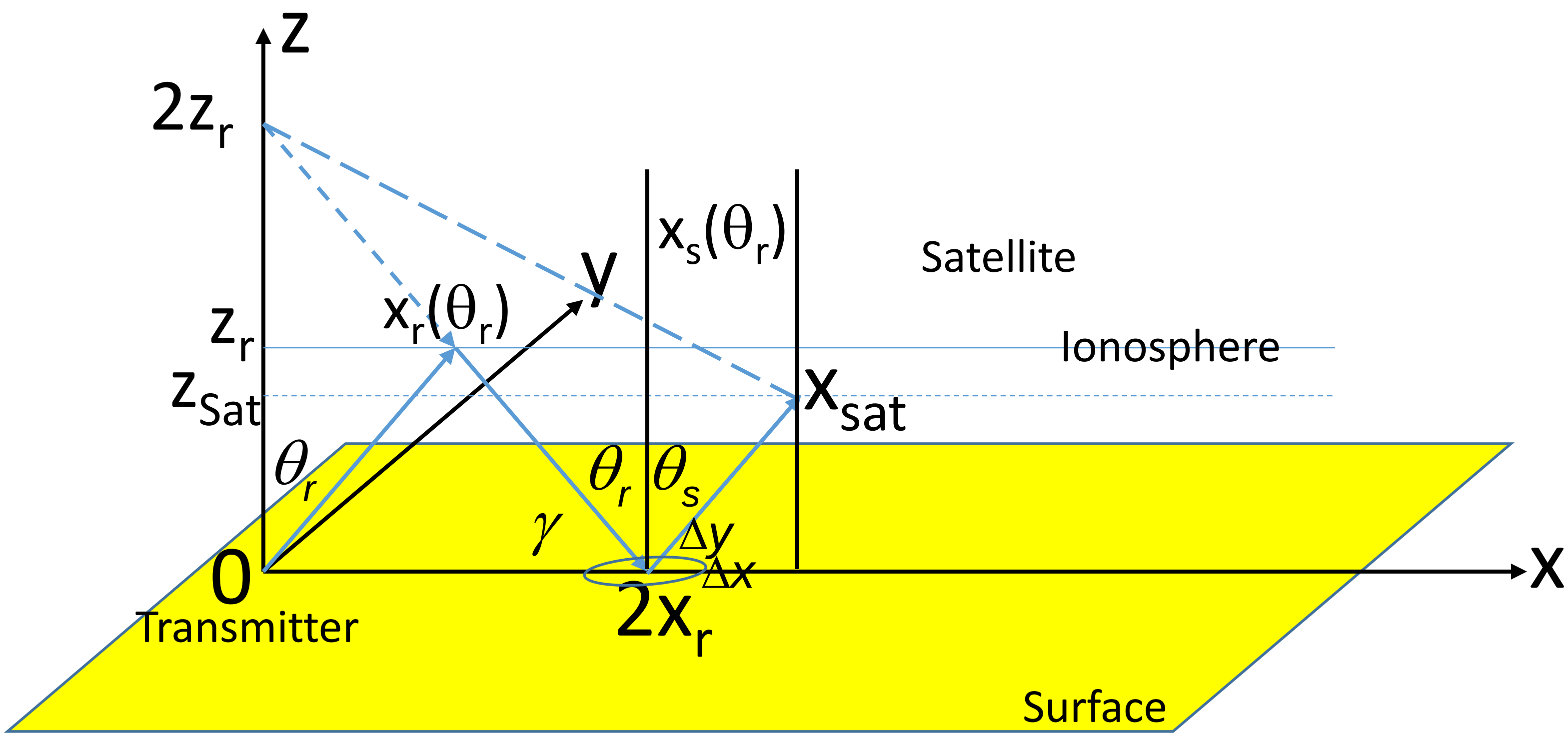

$$A_0 = \pi \, \Delta x \, \Delta y \, \square \, 10 \text{ km}^2$$

Ocean Scatter Angles and Power

- Incidence Zenith Angle: $\cos\theta_i = \hat{\mathbf{x}}_{Vertical} \cdot \hat{\mathbf{k}}_i$
- Scatter Zenith Angle: $\cos\theta_s = \hat{\mathbf{x}}_{Vertical} \cdot \hat{\mathbf{k}}_s$
- Scatter Azimuth Angle: $\tan\phi_s = (\hat{\mathbf{k}}_i \times \hat{\mathbf{k}}_s) \cdot \hat{\mathbf{x}}_{Vertical} \,/\, [\hat{\mathbf{k}}_i \cdot \hat{\mathbf{k}}_s - (\hat{\mathbf{k}}_i \cdot \hat{\mathbf{x}}_{Vertical})(\hat{\mathbf{k}}_s \cdot \hat{\mathbf{x}}_{Vertical})]$
- Vertical-Vertical Polarization Ocean Scatter Cross-Section

$$\sigma_{pq} = 4\pi k_0^4 \,|\, \alpha_{pq}^{I} \,|^2 \, S_k[k_0\sqrt{(\sin\theta_s\cos\phi_s - \sin\theta_i)^2 + (\sin\theta_s\sin\phi_s)^2}],(p,q) = (L,L) \text{ or } (L,R)$$

- Amplitude Along Direct Ray Path from Transmitter to Satellite

$$P_{TS} = \frac{W_T G_T}{4\pi \,|\, \mathbf{D}_{TS}^{(\theta_x,0)} \times \mathbf{D}_{TS}^{(0,\theta_y)} \,|}$$

- Amplitude of Ocean Signals
  - Path Divergence through Ionosphere to Ocean: $P_{TO} = \dfrac{W_T G_T}{4\pi D_{TO}^2}$
  - Ocean Scatter Power: $W_O = P_{TO}\sigma_{pq}\pi\Delta x\Delta y = \dfrac{W_T G_T \sigma_{pq}\pi\Delta x\Delta y}{4\pi D_{TO}^2}$
  - Ray Path Divergence Ocean to Satellite: $P_{OS} = \dfrac{W_O}{4\pi \,|\, \mathbf{D}_0^{(\theta_x,0)} \times \mathbf{D}_0^{(0,\theta_y)} \,|}$

Multiple Rays for Flat Earth with Biquadratic Layer

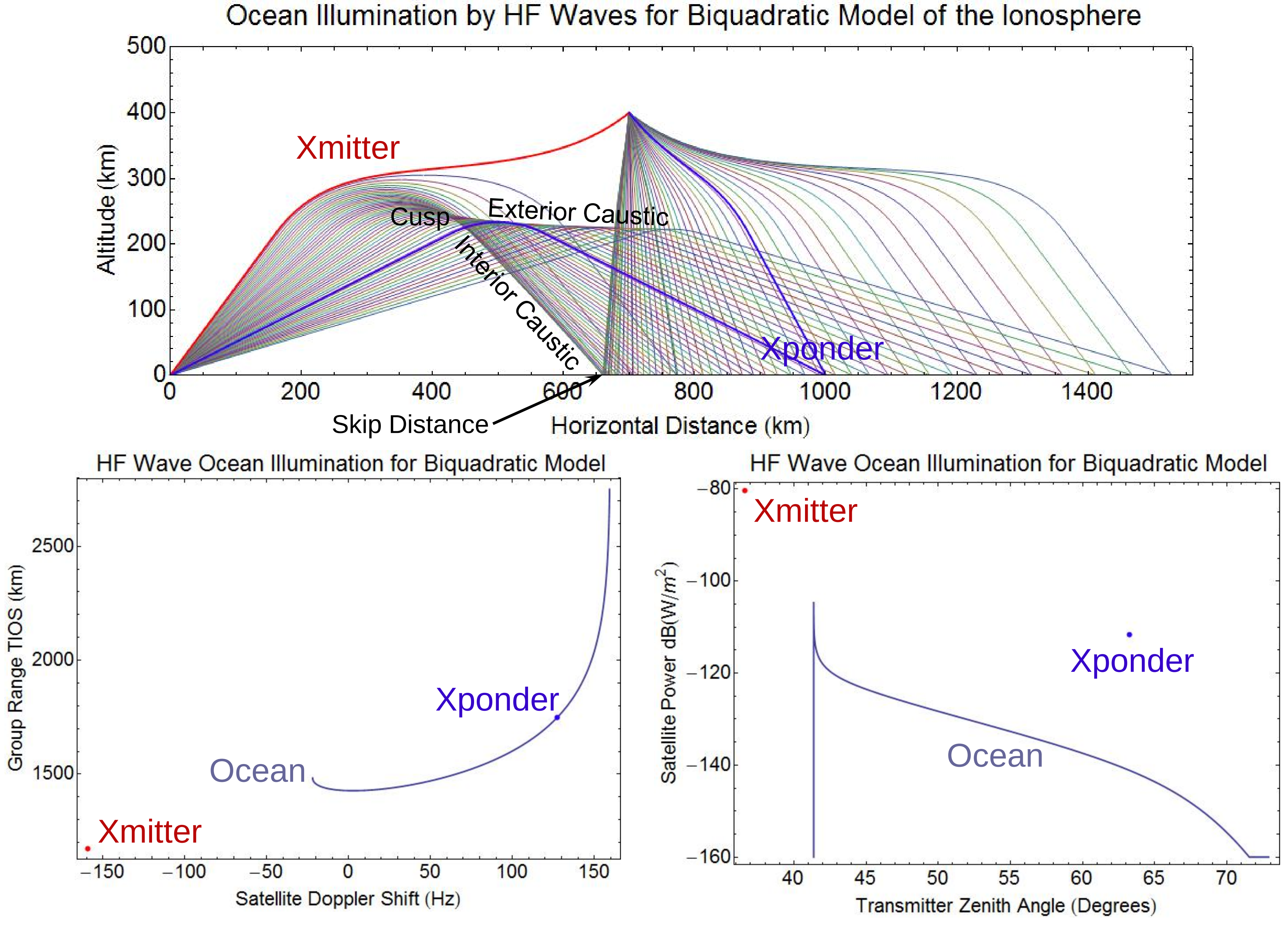

CASSIOPE Satellite with HF Receiver for Ocean Observations

ePOP Radio Receiver Instrument (RRI) Covers DC to 18 MHz Using 6-m Dipoles

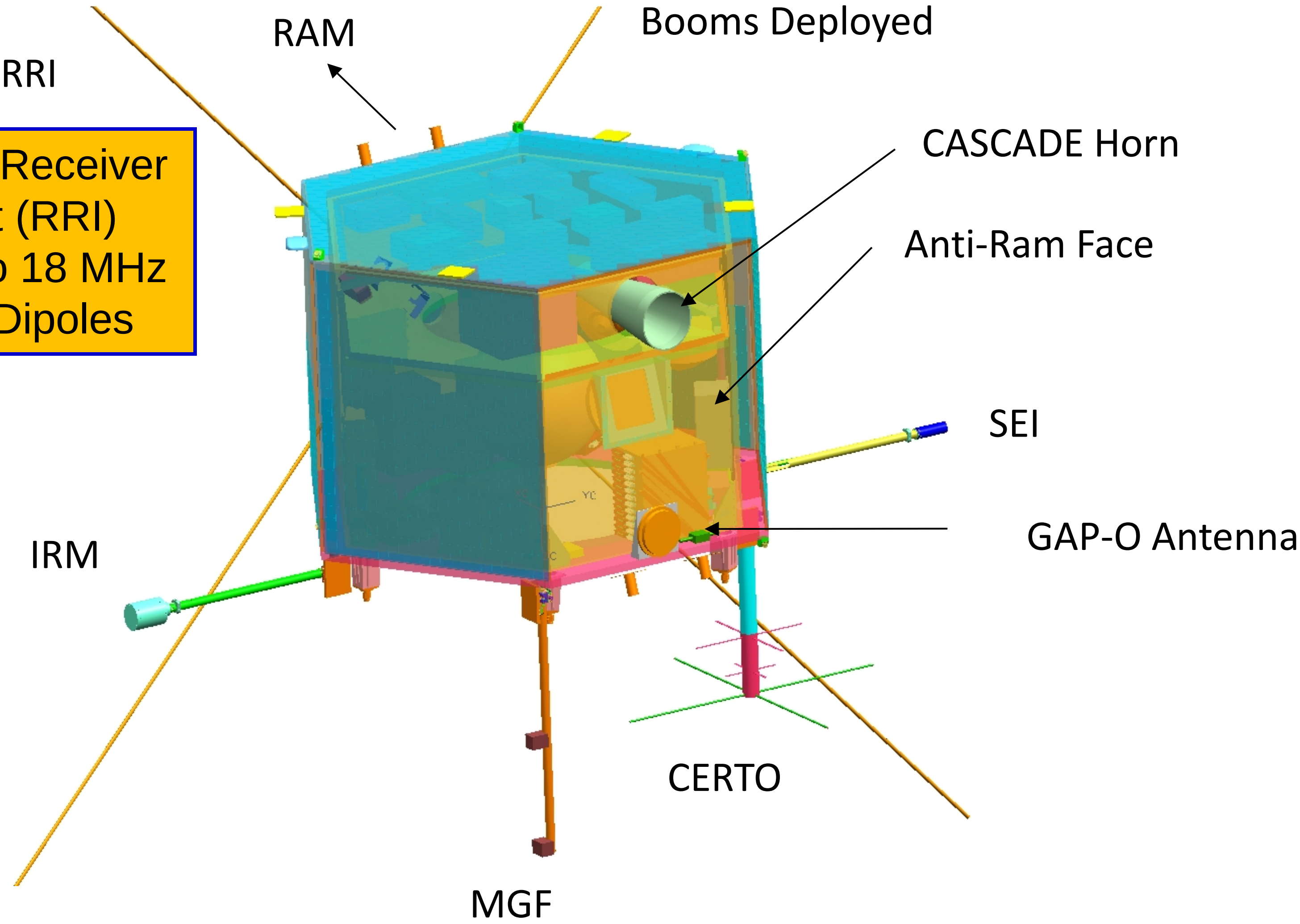

e-POP
Payload on Cassiope

13 April 2015 Ionograms and ePOP Orbit

FMCW Transmissions from ROTHR/VA at 17.5 MHz and Received by ePOP/RRI

62.5 Hz WRF

8.3 kHz Bandwidth

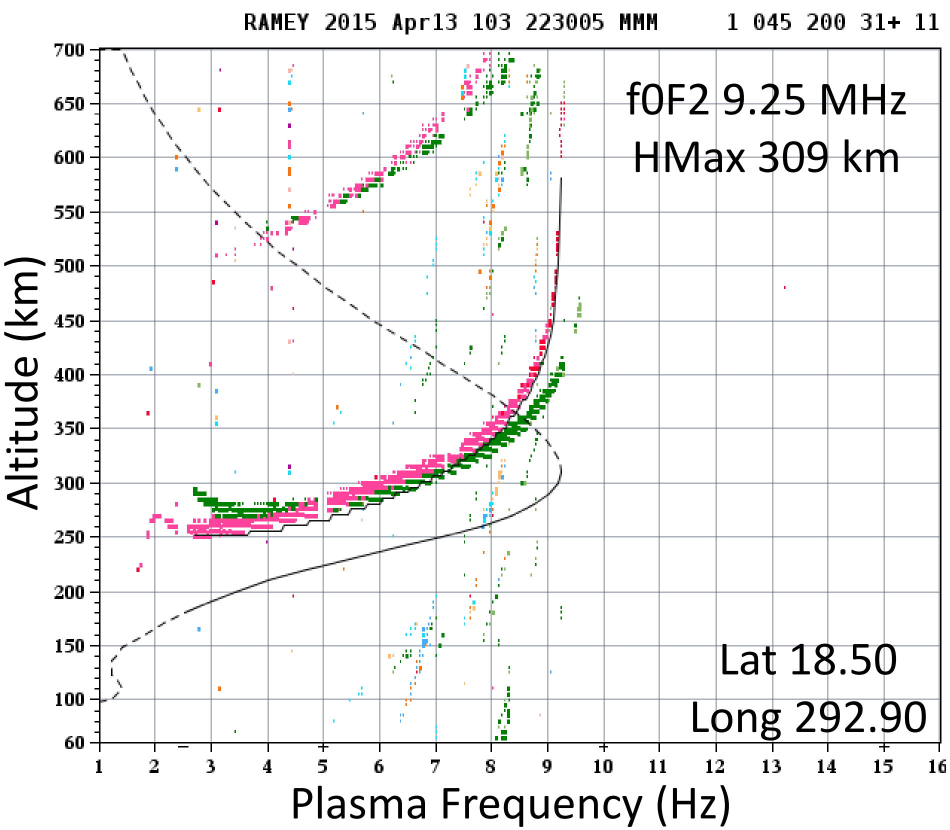

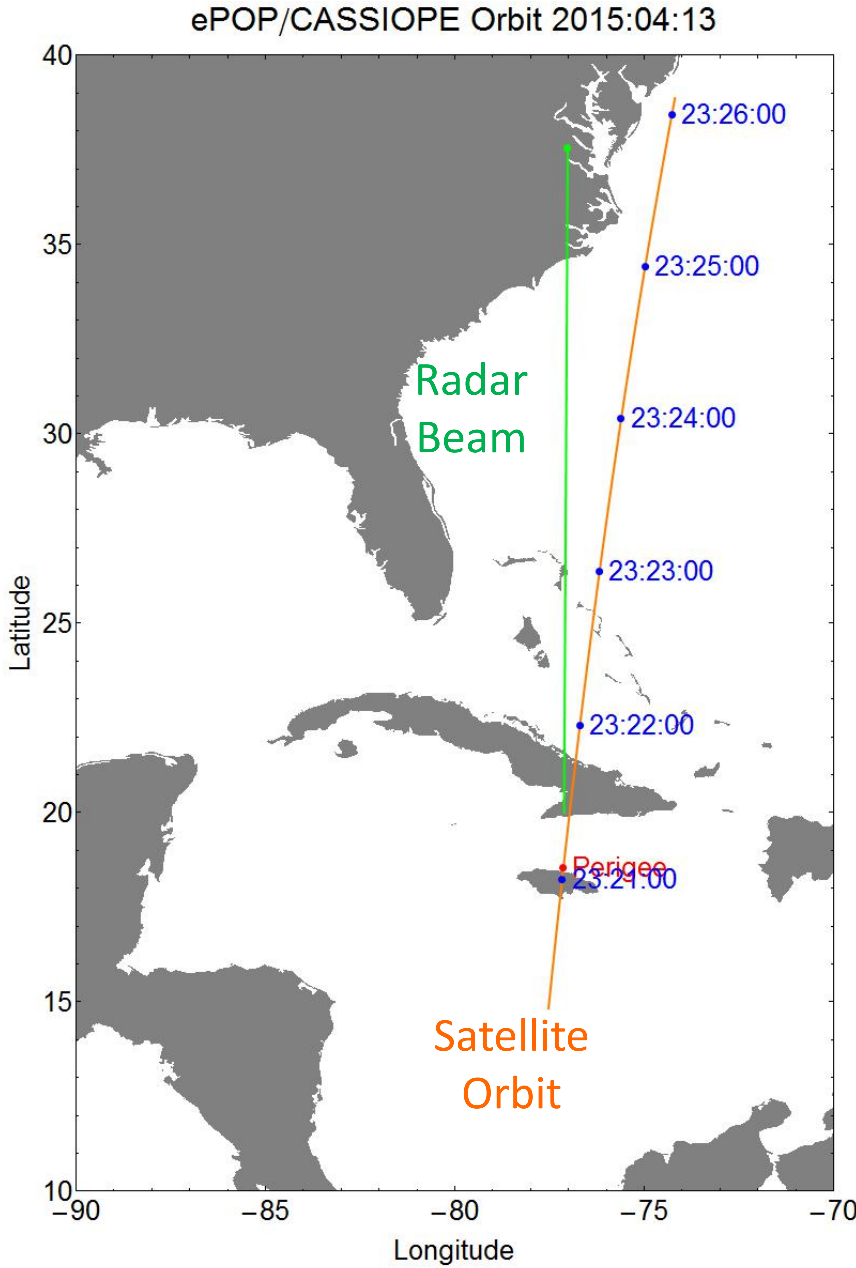

Range-Time Analysis of Radar Chirp

16 ms Chirp Period with 8.3 kHz Bandwidth

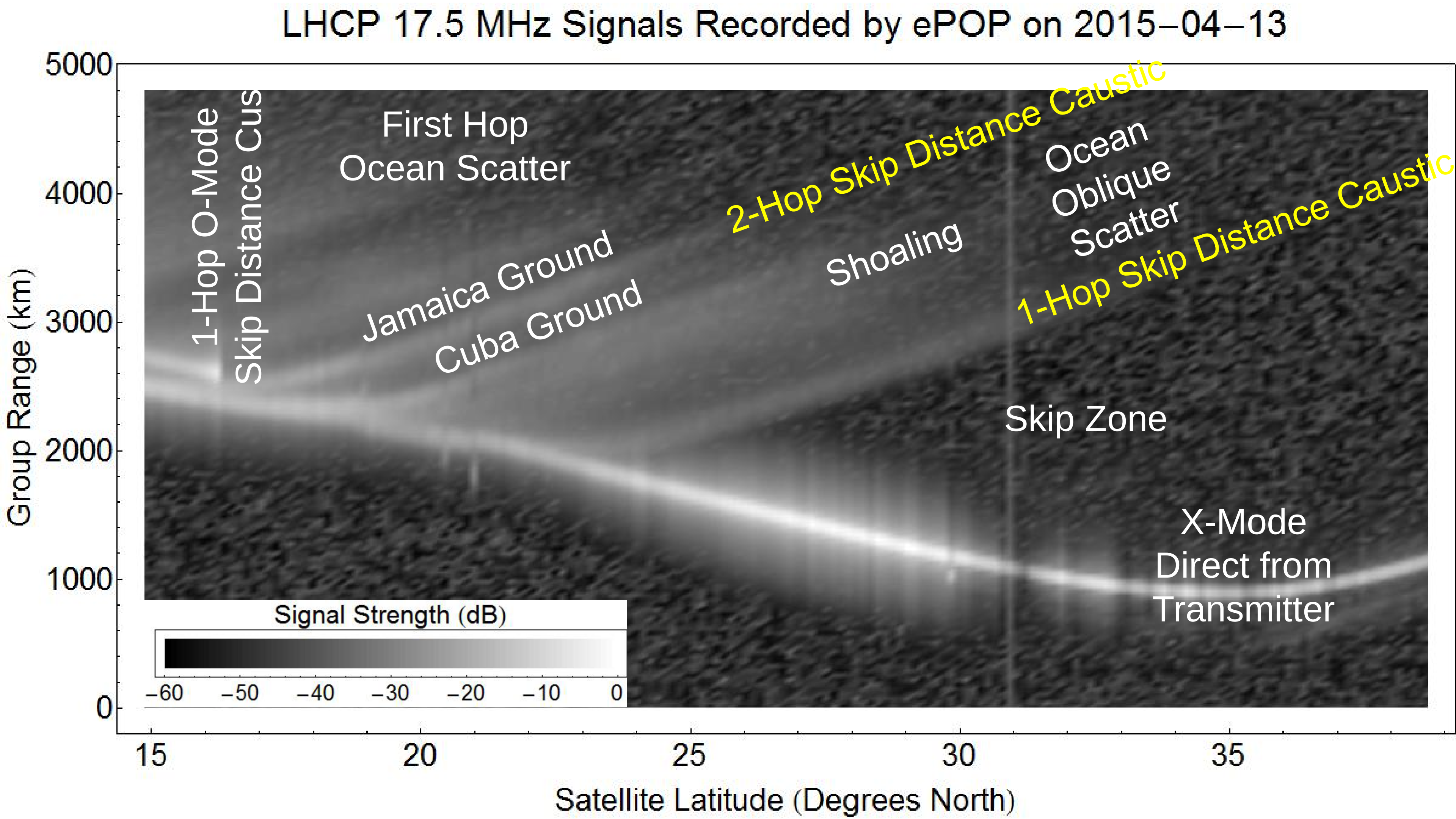

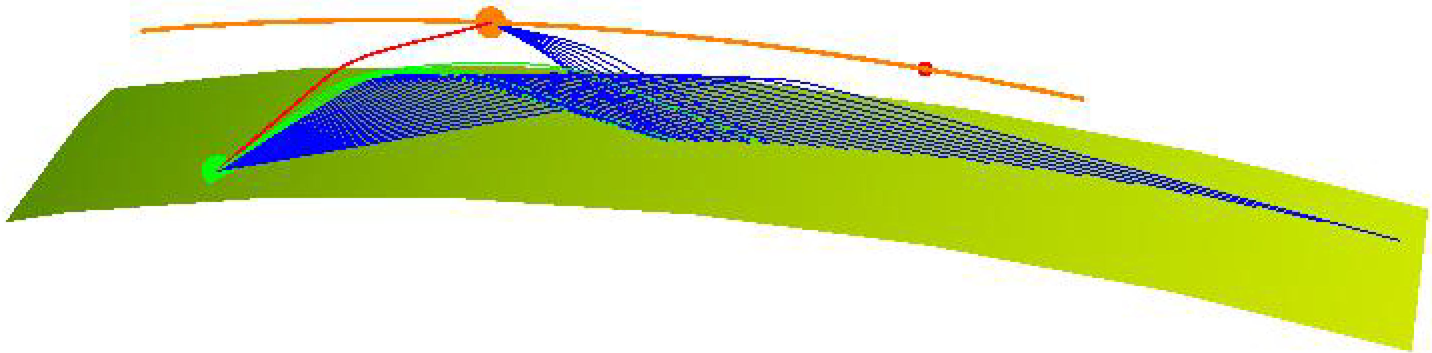

13 April 2015, 23:23:44

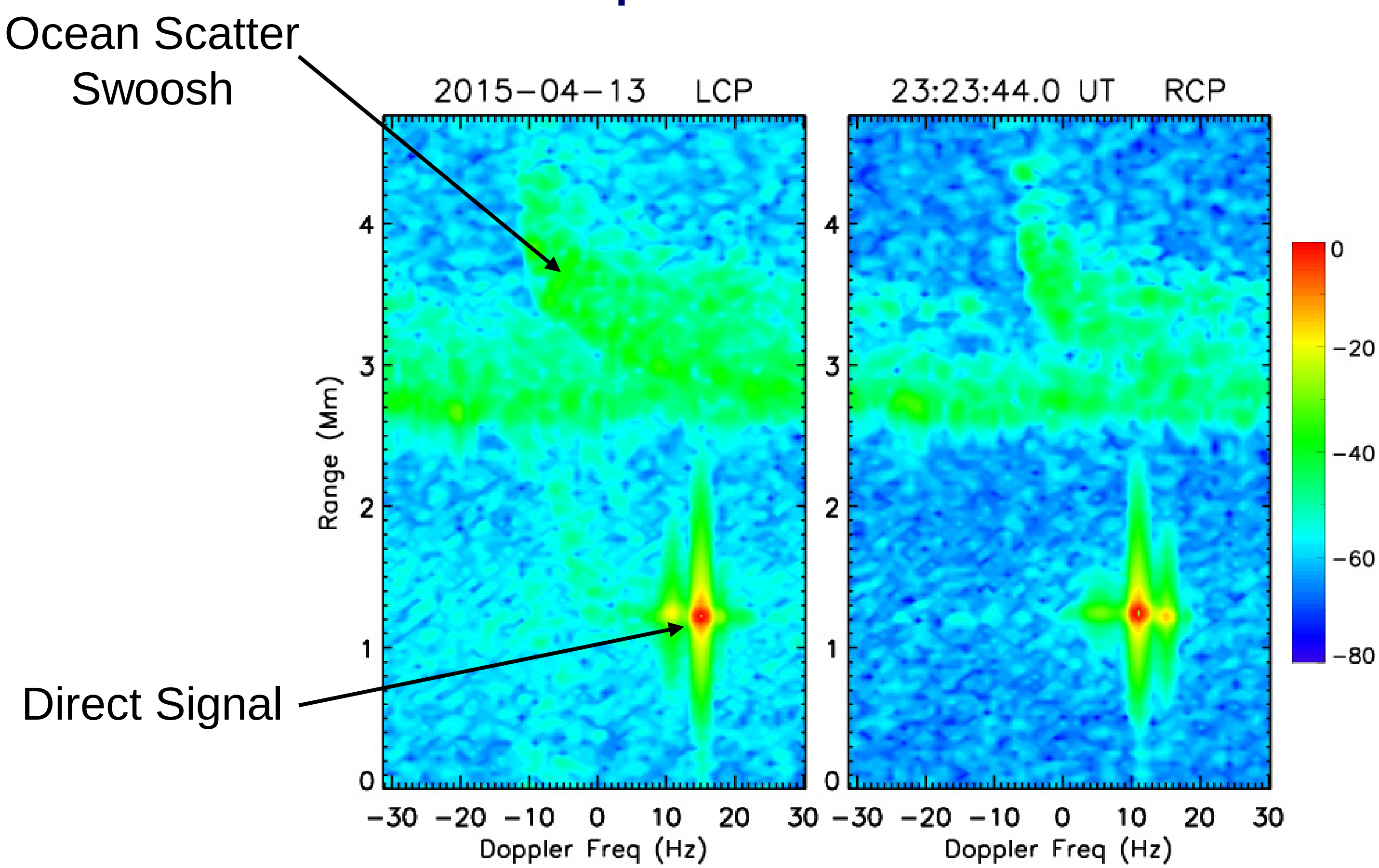

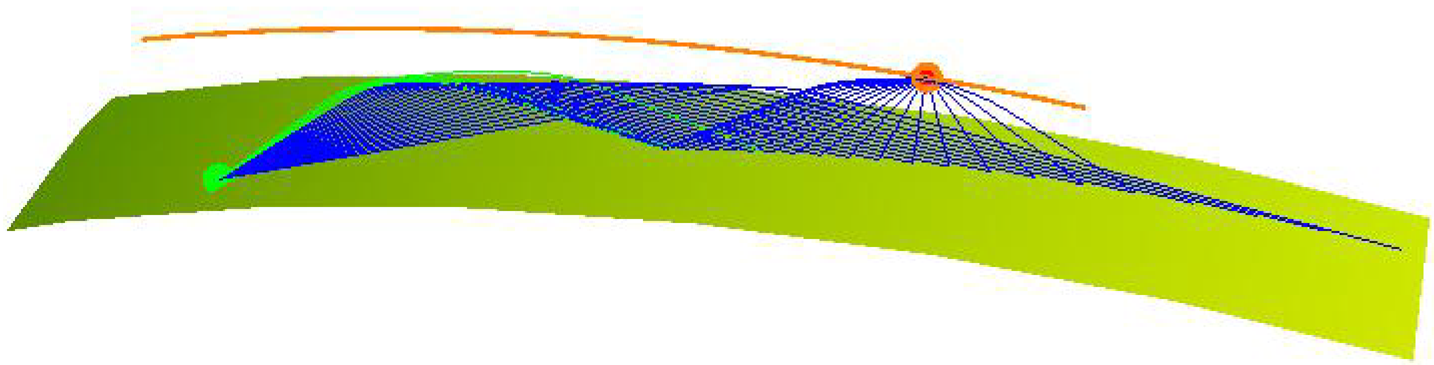

13 April 2015, 23:21:05

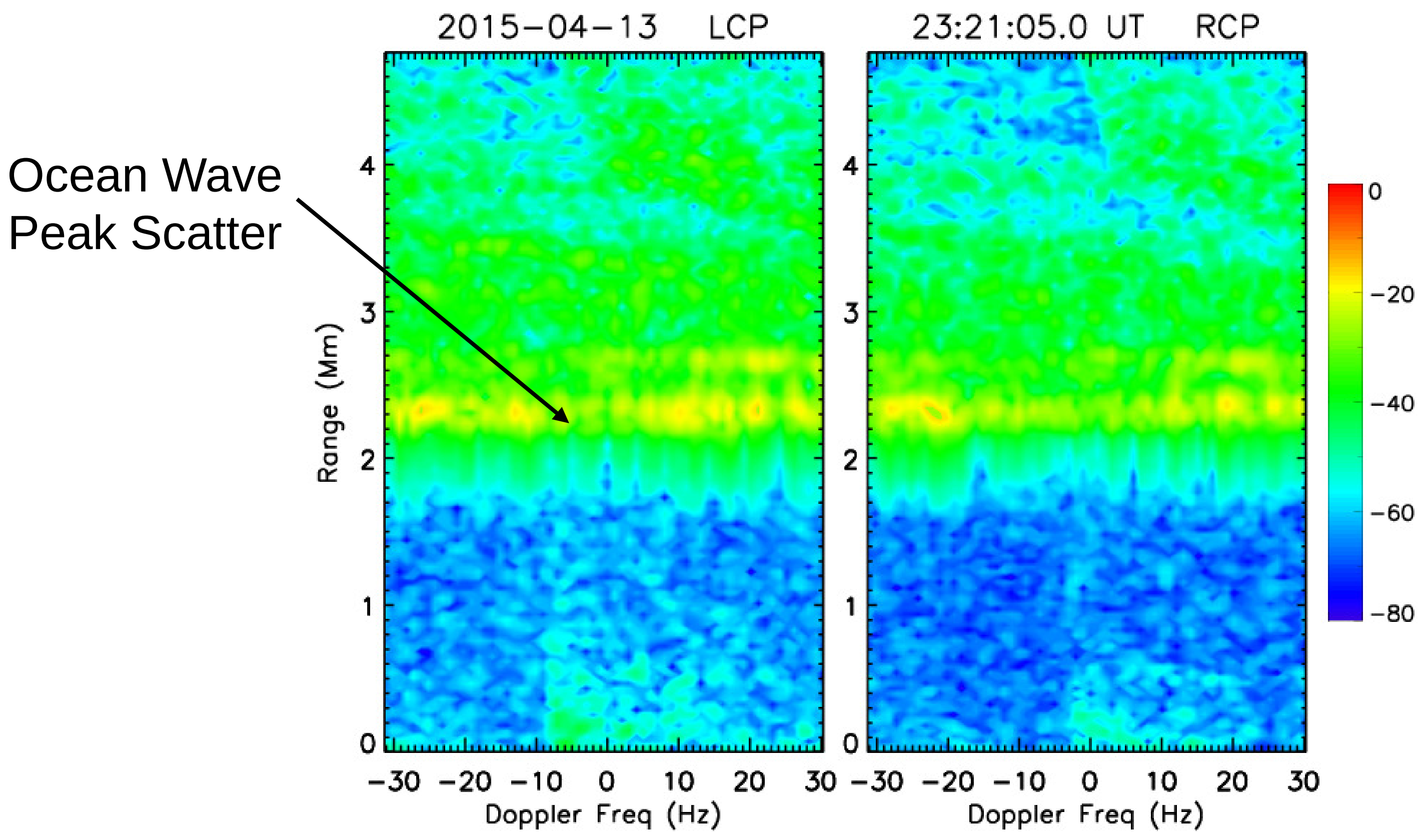

HF Transmission to Satellite by Direct and Ocean Scatter Paths

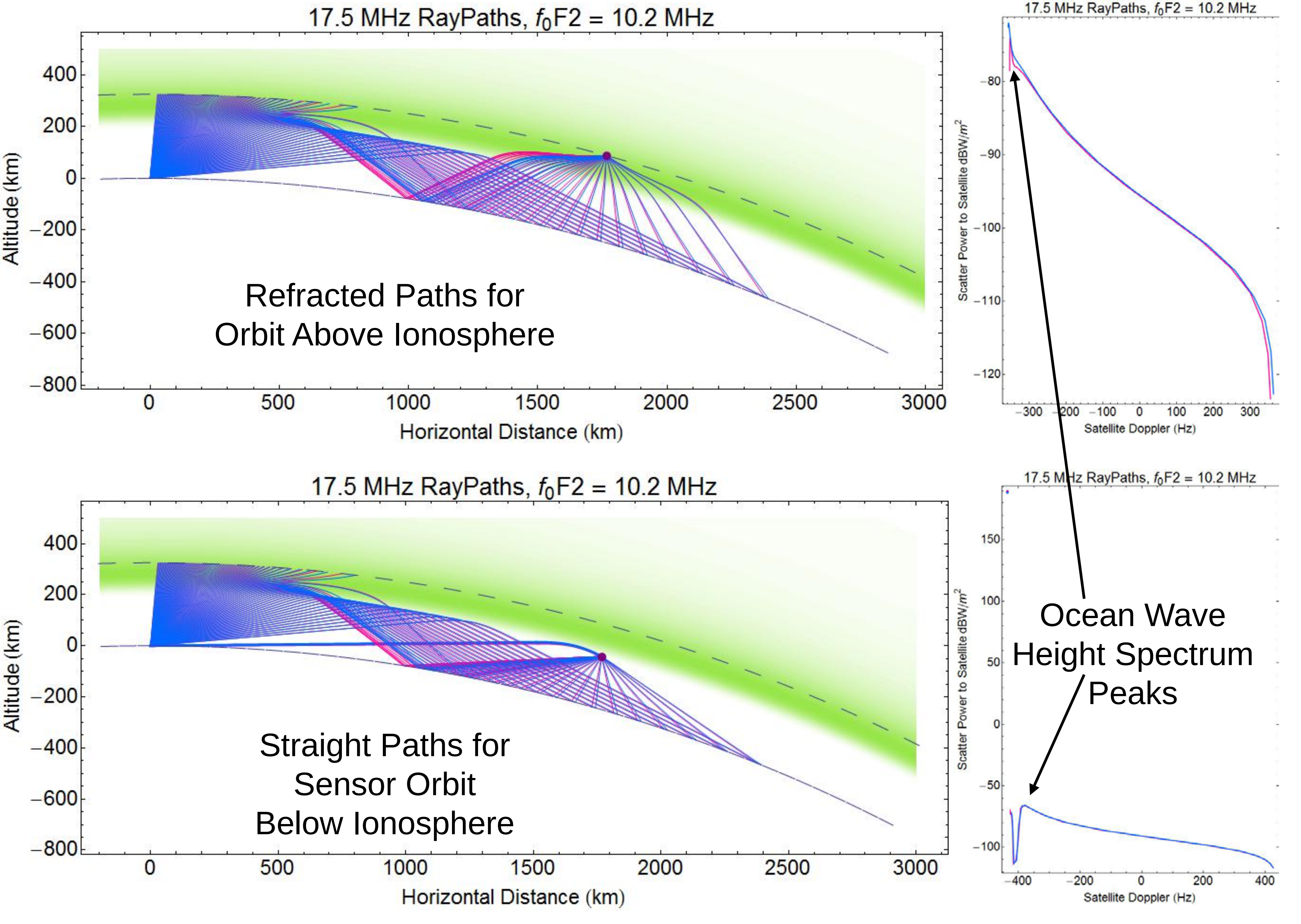

Naval Center for Space Technology
Plasma Physics Division
Naval Research Laboratory

Complex Action of Radio-Waves in the Ionosphere for Nonlinear Analysis (CARINA)

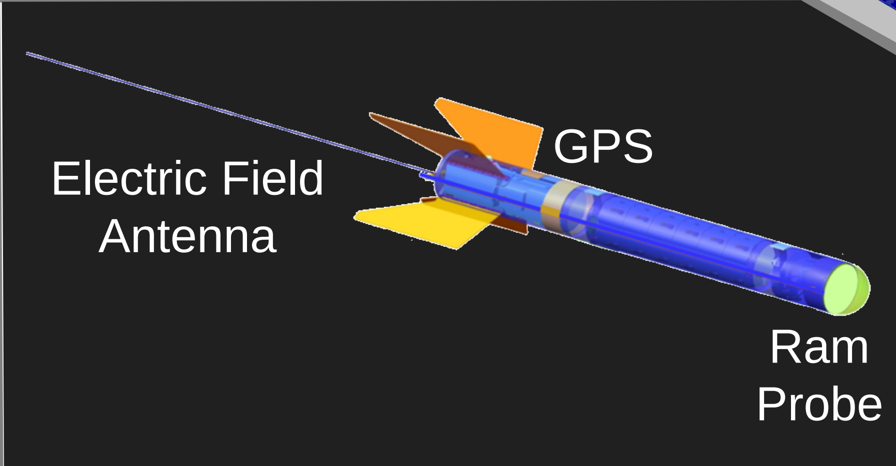

In Situ Investigation of the Lower Thermosphere

Government and Civilian Applications

- Provide Global Measurements of the Environment
  - World Coverage of E- and F-Regions
  - Storm Time Impacts on Radio Propagation
  - Coupling of Strong Lightning to Ionosphere
  - **Impact of Large Scale Ocean Disturbances**
  - Low Altitude Satellite Drag Coefficients
- Demonstrate Utility of Sub Ionosphere Orbit for Updating Operational Space Weather Models

TECHNICAL APPROACH and OBJECTIVES

- Unique Long Duration Satellite Flying Below the Ionosphere
  - **60 Day Orbit Between 150 and 270 km Altitude**
  - Low-Drag, Tubular Satellite (TubeSat)
- NRL Science Objectives
  - Directly Observe Electron Densities Below the F-Layer Peak
  - Sample Natural and Radio Electric Fields
  - Global Map of GPS TEC and Radio Scintillations
- Space Based Augmentation of Ground Facilities
  - Ionospheric Modification High Power Transmitters
  - UHF ISR, HF SuperDARN Radars, Ionosondes

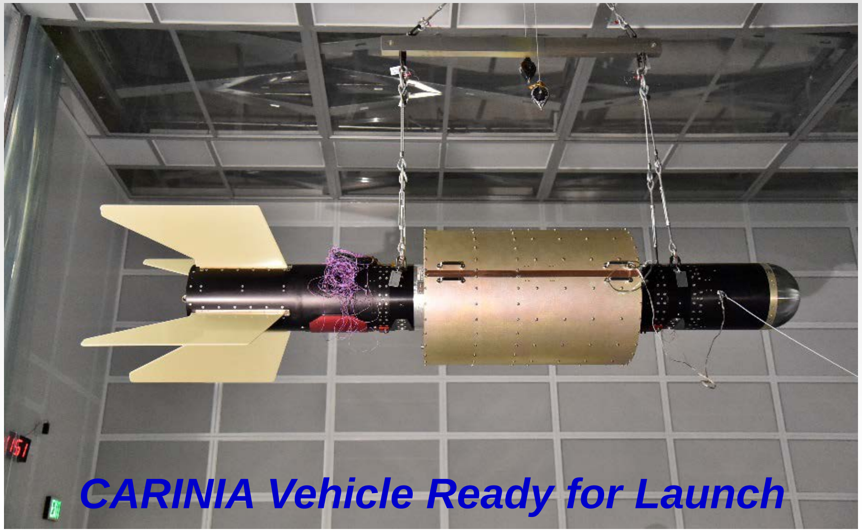

CARINIA Vehicle Ready for Launch

Naval Research Laboratory
Washington, DC 20375-5000

Contact: Paul Bernhardt, PI

Email: paul.bernhardt@nrl.navy.mil

Phone: (202) 767-0196

OTH Radar *Sky-Wave* Scatter from Ocean to ePOP and CARINA Satellites

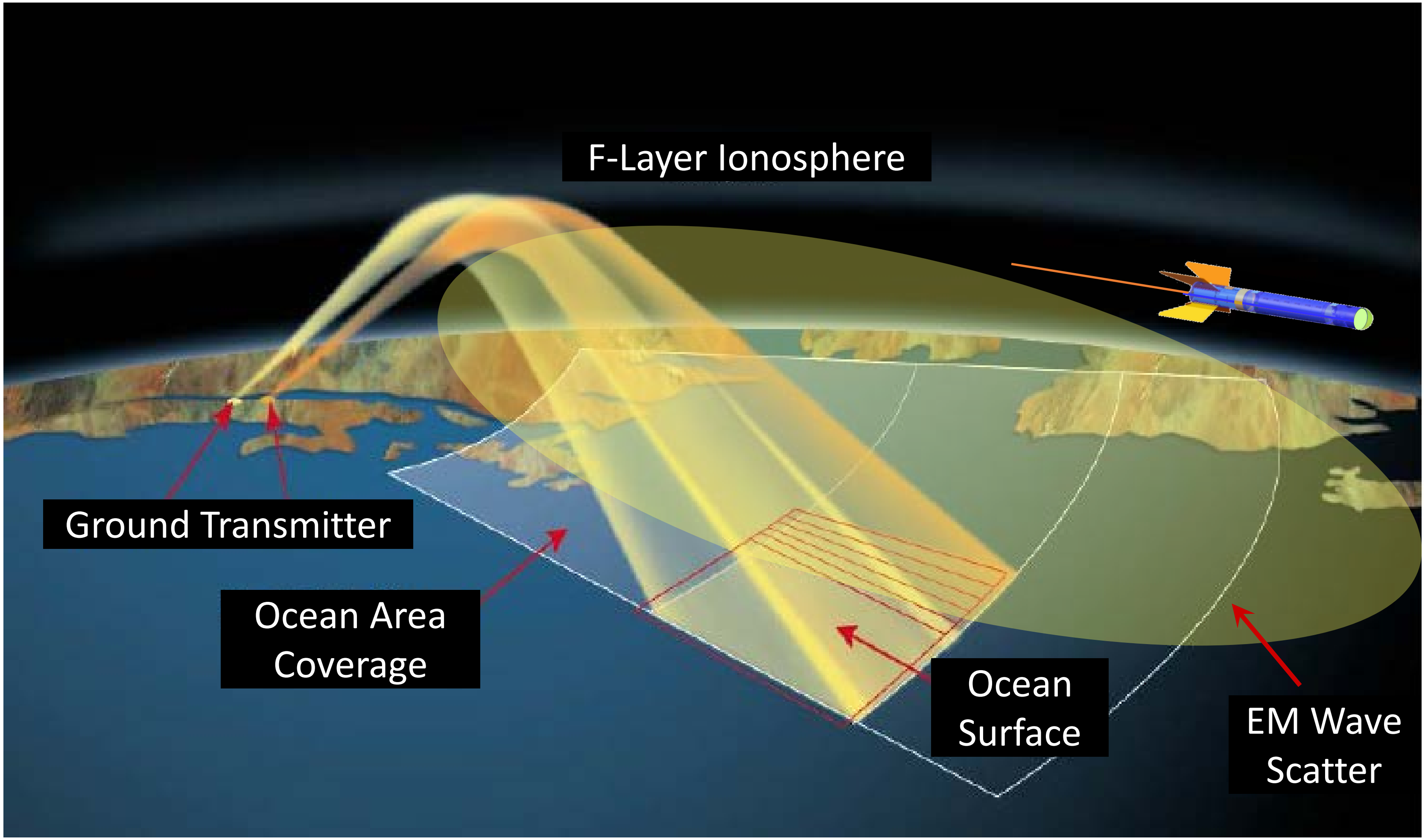

Great Improvement: HF Scatter to Receiver Below Ionosphere Removes Distortions

Simulated Swoosh for 4.8 MHz to a Receiver in a 200 km Orbit

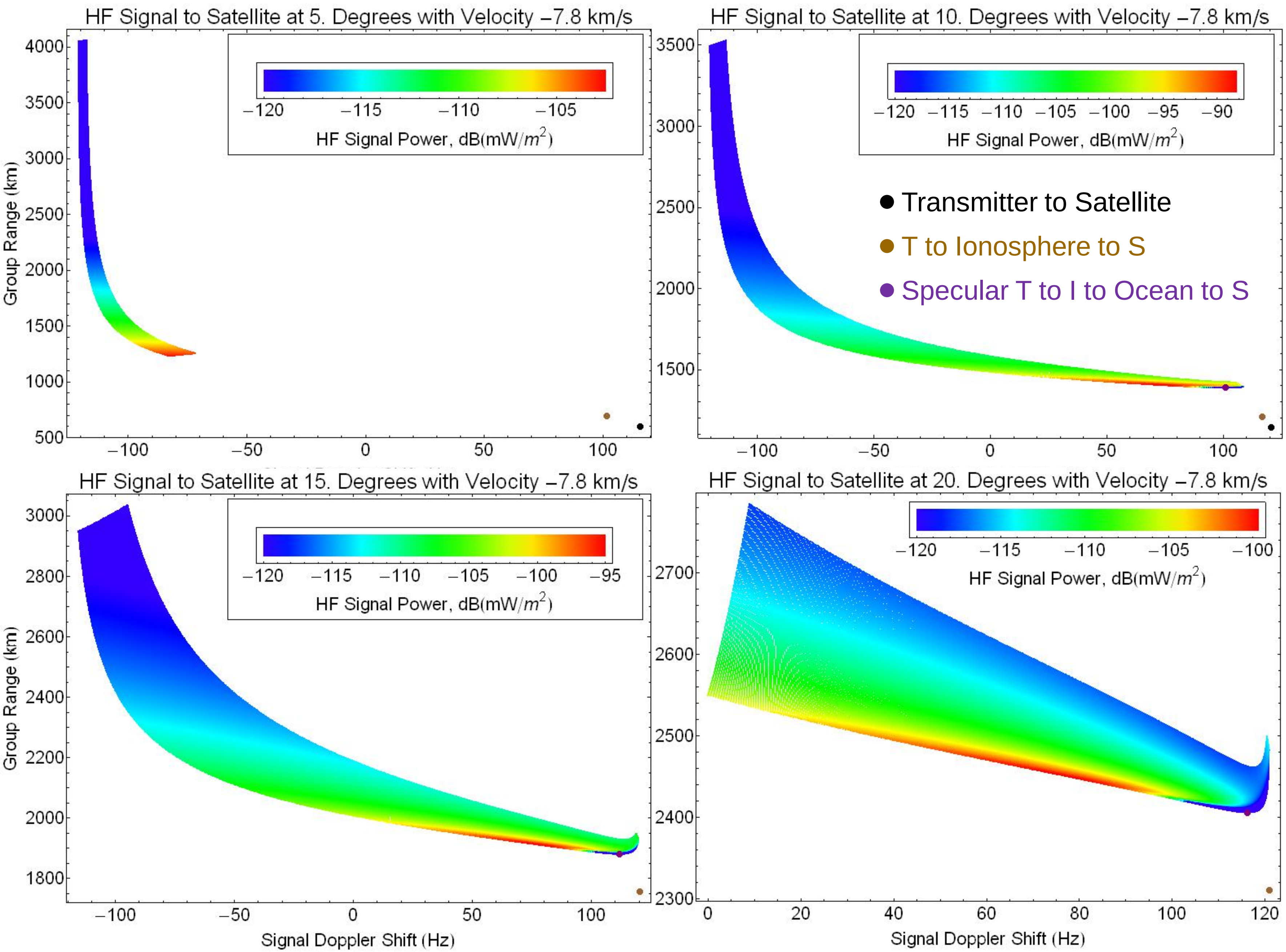

Ocean HF Scatter Conclusions

- HF Scatter and Ionosphere Propagation Tests
  - Single HF Transmitter Covers > 3000 km of Ocean Surface
  - Single Satellite Orbit Samples HF Illuminated Area
  - Brag Scatter from Ocean Through Ionosphere
  - Doppler Shifts and Group Delays Map to Ocean Surface
- Theory of Ocean Scatter
  - Coherent (Specular) and Incoherent (Bragg) Scatter
  - Bistatic Sampling of Global Ocean Surface
  - Realistic Models of Wave Height Spectrum Needed for Simulations
- Experimental Test with ROTHR/VA and ePOP/RRI
  - Data Collected in April and August 2015
  - Interpretation in Terms of Ocean Surface Parameters
- CARINA for 200 km Orbit
  - Program Delay Vehicle Assembly and Launch Selection
  - Planned Tests of the GOIS Concept After Launch